

# Radiation from Relativistic Strongly Magnetized Outflows

Vladimir V. Usov

*Department of Condensed Matter Physics, Weizmann Institute, Rehovot  
76100, Israel*

**Abstract.** Relativistic strongly magnetized winds outflowing from fast-rotating compact objects like millisecond pulsars with surface magnetic fields of  $\sim 10^{15} - 10^{16}$  G are plausible sources of cosmological  $\gamma$ -ray bursts. In such winds, there are at least three regions where extremely powerful X-ray and  $\gamma$ -ray emission may be generated. The first radiating region is the wind photosphere that is at a distance of  $\sim 10^9$  cm from the compact object. The second radiating region is at a distance of  $\sim 10^{13} - 10^{14}$  cm. In this region, the striped component of the wind field is transformed into large-amplitude electromagnetic waves. The third radiating region is at a distance of  $\sim 10^{16} - 10^{17}$  cm, where deceleration of the wind due to its interaction with an ambient medium becomes important. Radiation from all these regions is considered.

## 1. Introduction

Many ideas about the nature of  $\gamma$ -ray bursts have been discussed during last 25 years after the burst discovery (for a review, see Blaes 1994, Harding 1994, Hartman 1995; Dermer & Weiler 1995, Fishman & Meegan 1995, Greiner 1998, Piran 1998). Among these ideas, there was a suggestion that the sources of  $\gamma$ -ray bursts (GRBs) are at cosmological distances, i.e. at a redshift  $z \sim 1$  (Usov & Chibisov 1975, van den Berg 1983, Paczyński 1986, Goodman 1986, Eichler et al. 1989). After the BATSE data became available (Meegan et al. 1992, 1994), the idea of a cosmological origin of GRB sources has come to be taken very seriously (e.g., Paczyński 1991, Fishman & Meegan 1995). Recent detections of absorption and emission features at a redshift  $z = 0.835$  in the optical afterglow of GRB 970508 (Metzger et al. 1997) and at redshift  $z = 3.42$  in the host galaxy of GRB 971214 (Kulkarni et al. 1998) clearly demonstrate that at least some of the GRB sources lie at cosmological distances. A common feature of all acceptable models of cosmological  $\gamma$ -ray bursters is a relativistic wind as the source of GRB radiation. The Lorentz factor,  $\Gamma_0$ , of such a wind is about  $10^2 - 10^3$  or even more (e.g., Fenimore, Epstein & Ho 1993, Baring & Harding 1997). A very strong magnetic field may be in the plasma outflowing from cosmological  $\gamma$ -ray bursters (Usov 1992, 1994a,b, Thompson & Duncan 1993, Blackman, Yi & Field 1996, Vietri 1996, Katz 1997, Mészáros & Rees 1997a, Dai & Lu 1998). Below, we discuss both thermal and non-thermal radiation from relativistic strongly magnetized winds that are plausible sources of cosmological  $\gamma$ -ray bursters.

## 2. Relativistic strongly magnetized winds from cosmological $\gamma$ -ray bursters and their radiation: a plausible scenario

The energy output of cosmological  $\gamma$ -ray bursters in  $\gamma$ -rays typically is  $10^{51} - 10^{53}$  ergs (e.g., Wickramasinghe et al. 1993, Tamblyn & Melia 1993, Lipunov et al. 1995) and may be as high as  $3 \times 10^{53}$  ergs (Kulkarni et al. 1998) or even more (Kulkarni et al. 1999). These estimates assume isotropic emission of GRBs. Such a high energetics of cosmological  $\gamma$ -ray bursters and a short time scale of  $\gamma$ -ray flux variability call for very compact objects as sources of GRBs (Hartmann 1995, Piran 1998 and references therein). These objects may be either millisecond pulsars which are arisen from accretion-induced collapse of white dwarfs in close binaries (Usov 1992) or differentially rotating disk-like objects which are formed by the merger of a binary consisting of two neutron stars (Eichler et al. 1989, Narayan, Paczyński & Piran 1992). Such very young fast-rotating compact objects have two possible sources of energy which may be responsible for the radiation of cosmological GRBs. These are the thermal energy of the compact objects and the kinetic energy of their rotation. The thermal energy may be transformed into  $\gamma$ -rays by means of the following sequence of processes (for review, see Piran 1998): (1) Emission of neutrinos and cooling of the object; (2) Absorption of neutrinos ( $\nu_i + \bar{\nu}_i \rightarrow e^+ + e^-$ ) and formation of a fireball which mainly consists of electrons and positrons; (3) Expansion of the fireball and formation of a relativistic shell,  $\Gamma_0 > 10^2$ ; (4) Interaction of the shell with an external medium and acceleration of electrons to very high energies; and (5) Generation of  $\gamma$ -rays by highly accelerated electrons.

The maximum thermal energy,  $Q_{\text{th}}^{\text{max}}$ , of very young compact objects is high enough to explain the energy output of cosmological GBBs,  $Q_{\text{th}}^{\text{max}} \simeq$  a few  $\times 10^{53}$  ergs. However, the fraction of the thermal energy that is converted into the energy of the electron-positron fireball and then into the kinetic energy of the relativistic shell is very small and cannot be essentially more than  $10^{-3} - 10^{-2}$  (Goodman, Dar & Nussinov 1987, Eichler et al. 1989, Janka & Ruffert 1996, Piran 1998). Moreover, the efficiency of transformation of the kinetic energy of a relativistic shell into radiation cannot be more than 30 – 40% (Blandford & Eichler 1987). Therefore, neutrino powered winds outflowing from very young compact objects may be responsible for the radiation of cosmological GRBs only if they are well collimated, with opening angle about a few degrees or even less. For both neutron stars and post-merger objects, such a collimation of neutrino powered winds is very questionable (Woosley 1993, Piran 1998 and references therein).

The rotational energy of compact objects at the moment of their formation may be comparable with the thermal energy,  $Q_{\text{rot}}^{\text{max}} \simeq Q_{\text{th}}^{\text{max}}$ . The efficiency of transformation of the rotational energy to the energy of a relativistic strongly magnetized wind and then to the energy of high-frequency radiation may be as high as almost 100% (see Usov 1994a,b; Blackman et al. 1996 and below). For some time the theoretical expectation has been that rotation powered neutron stars (pulsars) should generate collimated outflows (e.g., Benford 1984, Michel 1985, Sulkanen & Lovelace 1990). The Crab, Vela, PSR B1509-58 and possible PSR B1951+32 all show evidence that this is indeed the case (Hester 1998, Gaensler et al. 1999 and references therein). If the energy flux from the source of GRB 990123 in the direction to the Earth is only about ten times more than the

energy flux averaged over all directions, the model of GRBs based on the rotation powered winds can easily explain the energetics of such an extremal event as GRB 990123 (Kulkarni et al. 1999). Such an anisotropy of emission from the burst sources doesn't contradict available data on GRBs (e.g., Perna & Loeb 1998). In the case of typical GRBs with the energy output of  $10^{51} - 10^{53}$  ergs, this model can explain their energetics even if the emission of GRBs is nearly isotropic. Therefore, the rotational energy of compact objects is a plausible source of energy for cosmological GRBs, not the thermal energy.

In many papers (e.g., Usov 1992, Thompson & Duncan 1993, Blackman et al. 1996; Kluźniak & Ruderman 1998), it was argued that the strength of the magnetic field  $B_s$  at the surface of compact objects may be as high as  $\sim 10^{16}$  G or even more. Such a strong magnetic field leads to both deceleration of the rotation of the compact object on a time scale of seconds and generation of a strongly magnetized wind that flows away from the object at relativistic speeds,  $\Gamma_0 \simeq 10^2 - 10^3$  (e.g., Usov 1994a). The outflowing wind is Poynting flux-dominated, i.e.,  $\sigma = L_{\pm}/L_P \ll 1$ , where

$$L_P \simeq \frac{2}{3} \frac{B_s^2 R^6 \Omega^4}{c^3} \simeq 2 \times 10^{52} \left( \frac{B_s}{10^{16} \text{ G}} \right)^2 \left( \frac{R}{10^6 \text{ cm}} \right)^6 \left( \frac{\Omega}{10^4 \text{ s}^{-1}} \right)^4 \text{ ergs s}^{-1} \quad (1)$$

is the luminosity of the compact object in the Poynting flux,  $L_{\pm}$  is its luminosity in both electron-positron pairs and radiation,  $c$  is the speed of light,  $R$  is the radius of the compact object and  $\Omega$  is its angular velocity;  $R \sim 10^6$  cm and  $\Omega \sim 10^4 \text{ s}^{-1}$  for both millisecond pulsars and post-merger objects. For compact objects with extremely strong magnetic fields,  $B_s \sim 10^{16}$  G, it is expected that  $\sigma$  is  $\sim 0.01 - 0.1$  (Usov 1994a).

A plausible magnetic topology for a relativistic magnetized wind outflowing from an oblique rotator ( $\vartheta \neq 0$ ) with a nearly dipole magnetic field is shown in Figure 1, where  $\vartheta$  is the angle between the rotational and magnetic axes. Near the rotational poles, the wind field should be helical (e.g., Coroniti 1990). This is because the magnetic flux originates in a single polar cap. Near the rotational equator, the toroidal magnetic field of the wind should be striped and alternates in polarity on a scalelength of  $\pi(c/\Omega) \sim 10^7$  cm. These magnetic stripes are separated by thin current sheets ( $J_{\theta}$ ). Off the equator, the magnetic flux in the toward and away stripes is unequal if  $\vartheta \neq \pi/2$ . In other words, in the striped region, the wind field is a superposition of a pure helical field and a pure striped field with nearly equal magnetic fluxes in adjacent stripes.

Since the luminosity of a  $\gamma$ -ray burster in a relativistic magnetized wind drops in time,  $L_P \propto t^{-\beta}$ , the wind structure at the moment  $t \gg \tau_{\Omega}$  is similar to a shell with the radius  $r \simeq ct$ , where  $\beta$  is a numerical index,  $1 \leq \beta \leq 2$ , and  $\tau_{\Omega} \sim 10^{-2} - 10^2$  s is the characteristic time of deceleration of the compact object rotation because of the action of the electromagnetic torque and the torque connected with the generation of gravitational radiation (Usov 1992, Yi & Blackman 1998). The thickness of the shell is  $\sim c\tau_{\Omega}$ . The strength of the magnetic field in the shell is about

$$B \simeq B_s \frac{R^3}{r_{\text{ic}}^2 r} \simeq 10^{15} \frac{R}{r} \left( \frac{B_s}{10^{16} \text{ G}} \right) \left( \frac{\Omega}{10^4 \text{ s}^{-1}} \right)^2 \text{ G}, \quad (2)$$

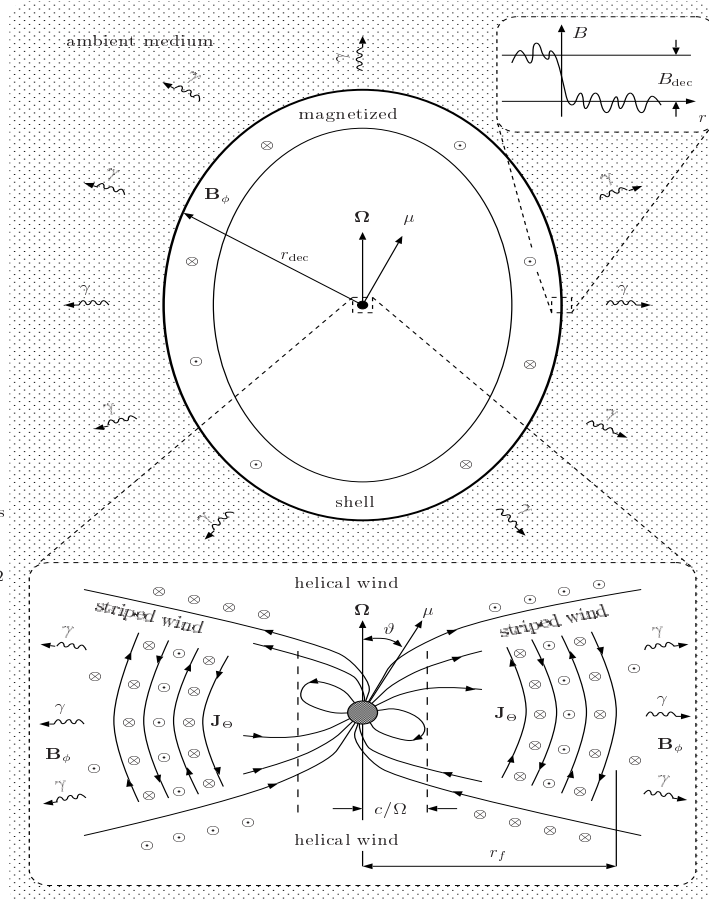


Figure 1. Sketch (not to scale) of the region where a cosmological GRB is generated by a relativistic, strongly magnetized wind. This wind is produced by a fast-rotating compact object like a millisecond pulsar with the angular velocity  $\Omega$  and the magnetic moment  $\mu$ .

where  $r_{lc} = c/\Omega = 3 \times 10^6 (\Omega/10^4 \text{ s}^{-1}) \text{ cm}$  is the radius of the light cylinder.

For relativistic, strongly magnetized winds with  $L_P \sim 10^{52} \text{ ergs s}^{-1}$  and  $\sigma \sim 0.01 - 0.1$ , the optical depth of the outflowing electron-positron plasma near the compact objects is very high, up to  $\sim 10^{12} - 10^{13}$  (Usov 1994a). In this case, the electron-positron plasma and radiation are in quasi-thermodynamic equilibrium. During outflow, the electron-positron plasma accelerates and its density decreases (e.g., Paczyński 1986, Goodman 1986). At a distance  $r_{ph}$  from the compact object, where the optical depth for the bulk of the photons is  $\sim 1$ , the radiation propagates freely. The radius of the wind photosphere is  $r_{ph} \sim 10^9 \text{ cm}$ , and the Lorentz factor of the outflowing plasma at the photosphere is  $\sim 10^2$  (see § 3).

At the distance

$$r < r_f \simeq 2 \times 10^{14} \sigma^{3/4} \left( \frac{B_s}{10^{16} \text{ G}} \right)^{1/2} \left( \frac{\Omega}{10^4 \text{ s}^{-1}} \right)^{1/2} \text{ cm}, \quad (3)$$

the magnetic field of the wind is frozen in the outflowing plasma (Usov 1994a, Blackman & Yi 1998), and there is no reason for powerful non-thermal radiation to be generated.

At  $r > r_f$ , the wind density is not sufficient to screen displacement currents, and the striped component of the wind field is transformed into large-amplitude electromagnetic waves (LAEMWs) (Usov 1975, 1994a,b, Blackman et al. 1996, Melatos & Melrose 1996a,b). Outflowing particles are accelerated in the field of LAEMWs and generate powerful synchro-Compton radiation (see § 4).

At  $r \gg r_f$ , the magnetic field is helical everywhere in the outflowing wind (see Fig. 1). Such a relativistic strongly magnetized wind expands more or less freely up to the distance

$$r_{dec} \simeq 5 \times 10^{16} \left( \frac{Q_{kin}}{10^{52} \text{ ergs}} \right)^{1/3} \left( \frac{n}{1 \text{ cm}^{-3}} \right)^{-1/3} \left( \frac{\Gamma_0}{10^2} \right)^{-2/3} \text{ cm}, \quad (4)$$

at which deceleration of the wind due to its interaction with an ambient medium becomes important (Rees & Mészáros 1992), where  $n$  is the density of the ambient medium and  $Q_{kin}$  is the kinetic energy of the outflowing wind,  $Q_{kin} \leq Q_{rot} \leq Q_{rot}^{max}$ .

It was suggested by Mészáros and Rees (1992, 1993) that in the process of the wind – ambient medium interaction at  $r \sim r_{dec}$ , an essential part of the wind energy may be transferred to high-energy electrons and then to high-frequency (X-ray and  $\gamma$ -ray) emission. This suggestion was recently confirmed by numerical simulations (see Smolsky & Usov 1996, 1999, Usov & Smolsky 1998 and § 5).

Summarizing, in relativistic strongly magnetized winds there are three regions where powerful radiation of GRBs may be generated. The first radiating region is the wind photosphere that is at the distance  $r_{ph} \sim 10^9 \text{ cm}$  from the compact object. The second radiating region is at the distance  $r_f \sim 10^{13} - 10^{14} \text{ cm}$ . In this region, the striped component of the wind field is transformed into LAEMWs. The third radiating region is at the distance  $r_{dec} \sim 10^{16} - 10^{17} \text{ cm}$  where deceleration of the wind due to its interaction with the ambient medium becomes important. Below, we consider radiation from all these regions.

### 3. Thermal radiation from the wind photosphere

For a spherical optically thick electron-positron wind, the radius of the photosphere is (Paczynski 1990)

$$r_{\text{ph}} \simeq \left( \frac{L_{\pm}}{4\pi a T_0^4 \Gamma_{\text{ph}}^2} \right)^{1/2}, \quad (5)$$

where  $T_0$  is the temperature of the electron-positron plasma at  $r \simeq r_{\text{ph}}$  in the comoving frame,  $a = 5.67 \times 10^{-5} \text{ ergs cm}^{-2} \text{ K}^{-4} \text{ s}^{-1}$  is the Stefan-Boltzmann constant, and  $\Gamma_{\text{ph}}$  is the mean Lorentz factor of the outflowing plasma at  $r \simeq r_{\text{ph}}$ .

Since  $\Gamma_{\text{ph}} \simeq r_{\text{ph}}/r_{\text{lc}}$  and  $T_0 \simeq 2 \times 10^8 \text{ K}$  (e.g., Paczynski 1986, Goodman 1986), from equation (5) we have (Usov 1994a)

$$r_{\text{ph}} \simeq \left( \frac{L_{\pm} r_{\text{lc}}^2}{4\pi a T_0^4} \right)^{1/4} \simeq 6 \times 10^8 \sigma^{1/4} \left( \frac{B_s}{10^{16} \text{ G}} \right)^{1/2} \left( \frac{\Omega}{10^4 \text{ s}^{-1}} \right)^{1/2} \text{ cm}, \quad (6)$$

$$\Gamma_{\text{ph}} \simeq 2 \times 10^2 \sigma^{1/4} \left( \frac{B_s}{10^{16} \text{ G}} \right)^{1/2} \left( \frac{\Omega}{10^4 \text{ s}^{-1}} \right)^{3/2}. \quad (7)$$

At  $r < r_{\text{ph}}$  the optical depth increases sharply with decreasing  $r$ . Therefore, any energy that is inherited by particles and radiation at the distance to the compact object a few times smaller than  $r_{\text{ph}}$  will be thermalized before it is radiated at  $r \simeq r_{\text{ph}}$ .

The temperature that corresponds to the blackbody-like radiation from the wind photosphere is

$$T_{\text{th}} \simeq 2\Gamma_{\text{ph}} T_0 \simeq 8 \times 10^{10} \sigma^{1/4} \left( \frac{B_s}{10^{16} \text{ G}} \right)^{1/2} \left( \frac{\Omega}{10^4 \text{ s}^{-1}} \right)^{3/2} \text{ K}. \quad (8)$$

The mean energy of thermal photons is  $\langle \varepsilon_{\text{th}} \rangle \simeq 3kT_{\text{th}}$ . For typical parameters of the wind sources,  $B_s \simeq 10^{16} \text{ G}$ ,  $\Omega \simeq 10^4 \text{ s}^{-1}$  and  $\sigma \simeq 0.01 - 0.1$ , we have  $\langle \varepsilon_{\text{th}} \rangle \simeq 1 \text{ MeV}$  within a factor of 2-3 or so.

For the outflowing electron-positron wind, the flux of particles at  $r > r_{\text{ph}}$  is (Paczynski 1990)

$$\dot{N}_{\pm} \simeq \frac{4\pi c r_{\text{ph}} \Gamma_{\text{ph}}^2}{\sigma_T}, \quad (9)$$

where  $\sigma_T = 6.65 \times 10^{-25} \text{ cm}^2$  is the Thomson cross-section. Equations (6), (7) and (9) yield

$$\dot{N}_{\pm} \simeq 10^{49} \sigma^{3/4} \left( \frac{B_s}{10^{16} \text{ G}} \right)^{3/2} \left( \frac{\Omega}{10^4 \text{ s}^{-1}} \right)^{7/2} \text{ s}^{-1}. \quad (10)$$

From equations (1), (7) and (10), we can see that the total energy flux of the wind in electron-positron pairs at  $r > r_{\text{ph}}$  is a very small part of the luminosity of the

compact object in both electron-positron pairs and radiation at the moment of its formation,  $m_e c^2 \Gamma_{\text{ph}} \dot{N}_{\pm} \simeq 10^{-7} L_{\pm}$ , where  $m_e$  is the electron mass. Therefore, the thermal luminosity,  $L_{\text{th}}$ , of the wind photosphere practically coincides with  $L_{\pm}$ .

#### 4. Non-thermal radiation from the region of transformation of the striped wind component into LAEMWs

At  $r \simeq r_{\text{ph}}$ , the density of the outflowing electron-positron plasma,

$$n_{\pm} = \frac{\dot{N}_{\pm}}{4\pi c r_{\text{ph}}^2} \simeq 7 \times 10^{19} \sigma^{1/4} \left( \frac{B_s}{10^{16} \text{ G}} \right)^{1/2} \left( \frac{\Omega}{10^4 \text{ s}^{-1}} \right)^{5/2} \text{ cm}^{-3}, \quad (11)$$

is essentially higher than the critical value (e.g., Goldreich & Julian 1969)

$$n_{\text{cr}} = \frac{\Omega B}{4\pi c e} \simeq 2 \times 10^{14} \sigma^{-1/4} \left( \frac{B_s}{10^{16} \text{ G}} \right)^{1/2} \left( \frac{\Omega}{10^4 \text{ s}^{-1}} \right)^{5/2} \text{ cm}^{-3}. \quad (12)$$

In this case, the magnetic field is frozed in the wind plasma. In the process of the plasma outflow, the plasma density decreases in proportion to  $r^{-2}$  while the critical density is  $\propto r^{-1}$ . At the distance  $r_f$  that is given by equation (3), the plasma density is equal to the critical density,  $n_{\pm} = n_{\text{cr}}$ . At  $r > r_f \sim 10^{13} - 10^{14}$  cm, the plasma density is not sufficient to screen displacement currents, and the striped component of the wind field is transformed into LAEMWs due to development of magneto-parametric instability (Usov 1975, 1994a,b, Blackman et al. 1996, Melatos & Melrose 1996a,b). The frequency of generated LAEMWs is equal to  $\Omega$ , and their amplitude is  $\sim B$ . Outflowing particles are accelerated in the field of LAEMWs to the Lorentz factor of  $\sim (L_p/m_e c^2 \dot{N}_{\pm})^{2/3} \sim 10^6$  and generate non-thermal synchro-Compton radiation with the typical energy of photons  $\langle \varepsilon_{\gamma} \rangle \sim \hbar \Omega (L_p/m_e c^2 \dot{N}_{\pm})^2 \sim 1$  MeV (Usov 1994a,b, Blackman et al. 1996, Blackman & Yi 1998), where  $\hbar \simeq 10^{-27}$  ergs s is the Planck constant. [For a review on acceleration of electrons in the fields of LAEMWs and synchro-Compton radiation see (Gunn & Ostriker 1971, Blumenthal & Tucker 1974).]

The radiative damping length for LAEMWs generated at  $r \sim r_f$  is a few orders of magnitude less than  $r_f$  (Usov 1994a). Therefore, at  $r \gg r_f$  LAEMWs decay almost completely, and their energy is transferred to high-energy electron-positron pairs and then to X-ray and  $\gamma$ -ray photons. It is worth noting that in the case when the magnetic axis is perpendicular to the rotational axis,  $\vartheta = \pi/2$ , the electromagnetic field of the Poynting flux-dominated wind is purely striped just as vacuum magnetic dipole waves (Michel 1971), and almost all energy of the wind is radiated in X-rays and  $\gamma$ -rays at  $r \sim r_f$  (Usov 1994a, Blackman et al. 1996, Blackman & Yi 1998). In this case, the total energy output in hard photons per a GRB may be as high as  $Q_{\text{rot}}^{\text{max}} \simeq \text{a few} \times 10^{53}$  ergs.

At  $\vartheta \simeq \pi/2$ , when the bulk of the wind energy is transferred into  $\gamma$ -rays at  $r \sim r_f$  and the residual energy of the wind at  $r \gg r_f$  is small, afterglows which are generated at  $r > r_{\text{dec}} \gg r_f$  and accompany GRBs are weak irrespective of

that the GRBs themselves may be quite strong. This may explain the fact that X-ray, optical and radio afterglows have been observed in some strong GRBs but not in others (e.g., Piran 1998 and references therein).

## 5. Non-thermal radiation from the region of the wind – ambient medium interaction

For consideration of the interaction between a relativistic magnetized wind and an ambient medium, it is convenient to switch to the co-moving frame of the outflowing plasma (the wind frame). While changing the frame, the magnetic and electric fields in the wind are reduced from  $B$  and  $E = B[1 - (1/\Gamma_0^2)]^{1/2} \simeq B$  in the frame of the  $\gamma$ -ray burster to  $B_0 \simeq B/\Gamma_0$  and  $E_0 = 0$  in the wind frame. Using this and equations (2) and (4), for typical parameters of both cosmological  $\gamma$ -ray bursters,  $B_s \simeq 10^{16}$  G,  $\Omega \simeq 10^4$  s $^{-1}$ ,  $Q_{\text{kin}} \simeq 10^{52} - 10^{53}$  ergs and  $\Gamma_0 \simeq 10^2 - 10^3$ , and the ambient medium,  $n \simeq 1 - 10^2$  cm $^{-3}$ , we have that at  $r \simeq r_{\text{dec}}$  the strength of the magnetic field at the wind front is  $B_{\text{dec}} \simeq 10^4 - 4 \times 10^5$  G in the burster frame and  $B_0 \simeq B_{\text{dec}}/\Gamma_0 \simeq 10^2 - 10^3$  G in the wind frame.

In the wind frame, the problem of the wind – ambient medium interaction is identical to the problem of collision between a wide relativistic beam of cold plasma and a region with a strong magnetic field which is called a magnetic barrier. Recently, the interaction of a wide relativistic plasma beam with a magnetic barrier was studied numerically (Smolsky & Usov 1996, 1999, Usov & Smolsky 1998). In these studies, the following initial condition of the beam – barrier system was assumed. Initially, at  $t = 0$ , the ultrarelativistic homogenous neutral beam of protons and electrons (number densities  $n_p = n_e \equiv n_0$ ) runs along the  $x$  axis and impacts at the barrier, where  $n_0$  is constant. The beam is infinite in the  $y - z$  dimensions and semi-infinite in the  $x$  dimension. The magnetic field of the barrier  $\mathbf{B}_0$  is uniform and transverse to the beam velocity,  $\mathbf{B}_0 = B_0 \hat{\mathbf{e}}_z \Theta[x]$ , where  $B_0$  is constant and  $\Theta[x]$  is the step function equal to unity for  $x > 0$  and to zero for  $x < 0$ . At the front of the barrier,  $x = 0$ , the surface current  $J_y$  runs along the  $y$  axis to generate the jump of the magnetic field. The value of this current per unit length of the front across the current direction is  $cB_0/4\pi$ . A 1 $\frac{1}{2}$ D time-dependent solution for the problem of the beam – barrier interaction was constructed, i.e., electromagnetic fields ( $\mathbf{E} = E_x \hat{\mathbf{e}}_x + E_y \hat{\mathbf{e}}_y$ ;  $\mathbf{B} = B \hat{\mathbf{e}}_z$ ) and motion of the beam particles in the  $x - y$  plane were found. The field structure and the beam particle motion were treated self-consistently except the external current  $J_y$  which is fixed in our simulations.

The main results of our simulations are the following (Smolsky & Usov 1996, Usov & Smolsky 1998).

1. When the energy densities of the beam and the magnetic field,  $\mathbf{B}_0$ , of the barrier are comparable,

$$\alpha = 8\pi n_0 m_p c^2 (\Gamma_0 - 1) / B_0^2 \sim 1, \quad (13)$$

where  $m_p$  is the proton mass, the process of the beam – barrier interaction is strongly nonstationary, and the density of outflowing protons after their reflection from the barrier is strongly non-uniform. The ratio of the maximum density of reflected protons and their minimum density is  $\sim 10$ .

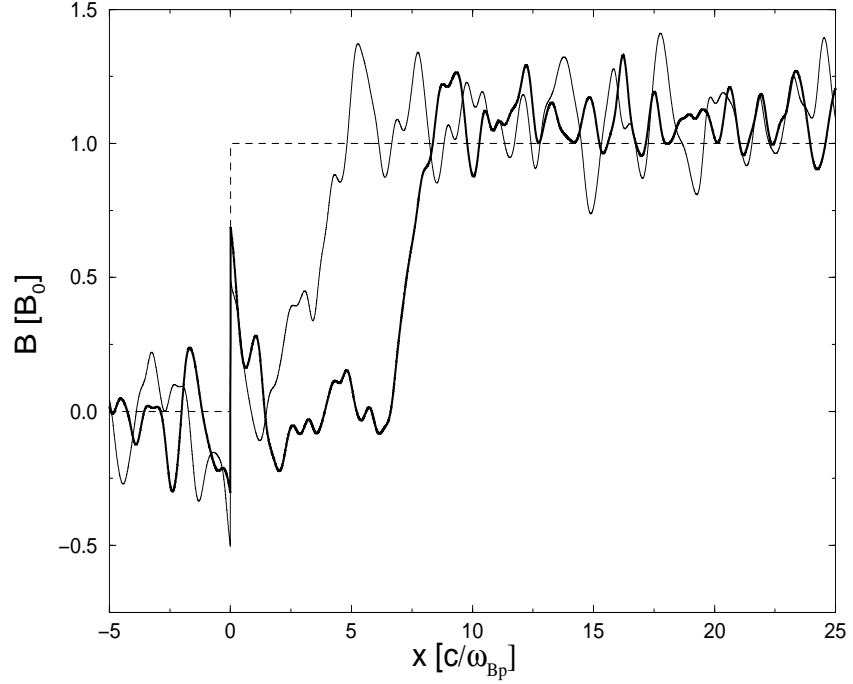


Figure 2. Distribution of magnetic field for a simulation with  $B_0 = 300$  G,  $\Gamma_0 = 300$  and  $\alpha = 2/3$  at the moments  $t = 0$  (dotted line),  $t = 7.96T_p$  (thin solid line), and  $t = 15.9T_p$  (thick solid line).  $T_p = 2\pi/\omega_{Bp}$  is the proton gyroperiod in the magnetic field,  $B_0$ , of the barrier.

2. At  $\alpha > \alpha_{\text{cr}} \simeq 0.4$ , the depth of the beam particle penetration into the barrier increases in time,  $x_{\text{pen}} \simeq v_{\text{pen}}t$ , where  $v_{\text{pen}}$  is the mean velocity of the penetration into the barrier. The value of  $v_{\text{pen}}$  is subrelativistic and varies from zero (no penetration) at  $\alpha \leq \alpha_{\text{cr}}$  to  $0.17c$  at  $\alpha = 1$  and  $0.32c$  at  $\alpha = 2$ . At  $\alpha > \alpha_{\text{cr}}$ , the magnetic field of the barrier at the moment  $t$  roughly is  $B(t) \simeq B_0\Theta[x - x_{\text{pen}}(t)]$  (see Fig. 2). In other words, the front of the beam – barrier interaction is displaced into the barrier with the velocity  $v_{\text{pen}}$ . For  $\alpha > \alpha_{\text{cr}}$ , our consideration of the beam – barrier interaction in the vicinity of the new front,  $x \simeq x_{\text{pen}}$ , is *completely self-consistent*, and no simplifying assumptions besides geometrical ones are exploited.

3. At the front of the barrier,  $x \simeq x_{\text{pen}}(t)$ , the surface current varies in time because of strong nonstationarity of the beam – barrier interaction at  $\alpha \sim 1$ , and LAEMWs are generated (Fig. 2). The frequency of these waves is about the proton gyrofrequency  $\omega_{Bp} = eB_0/m_p c \Gamma_0$  in the field of the barrier  $B_0$ . The wave amplitude  $B_w$  can reach  $\sim 0.2B_0$ .

4. At  $\alpha \sim 1$ , strong electric fields are generated in the vicinity of the front of the barrier,  $x \simeq x_{\text{pen}}(t)$ , and electrons of the beam are accelerated in these fields up to the mean energy of protons, i.e. up to  $\sim m_p c^2 \Gamma_0$  (Fig. 3). At  $\alpha_{\text{cr}} < \alpha < 1$ , the mean Lorentz factor of outflowing high-energy electrons after their reflection and acceleration at the barrier front depends on  $\alpha$  and is

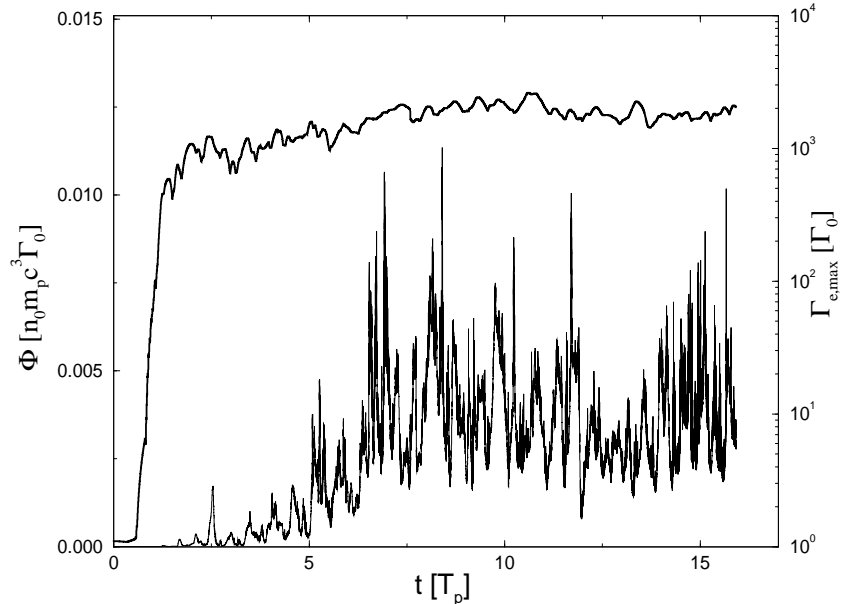


Figure 3. Maximum energy of accelerated electrons (thick line) and intensity of their synchrotron radiation per unitary area of the front of the magnetic barrier (thin line) in a simulation with  $B_0 = 300$  G,  $\Gamma_0 = 300$  and  $\alpha = 2/3$ .

$$\langle \Gamma_e^{\text{out}} \rangle \simeq 0.2 \left( \frac{m_p}{m_e} \right) \Gamma_0 \quad (14)$$

within a factor of 2. The total energy of the accelerated electrons is about 20% of the energy in the outflowing protons which are reflected from the magnetic barrier.

5. At  $\alpha_{\text{cr}} < \alpha < 1$ , the mean Lorentz factor of protons reflected from the barrier is  $\langle \Gamma_p^{\text{out}} \rangle \simeq (0.7 \pm 0.1) \Gamma_0$ , i.e. the process of the beam proton reflection from the barrier is non-elastic, and about 30% of the initial kinetic energy of the beam protons is lost in this collision. The energy that is lost by the beam protons is transferred to high-energy electrons and LAEMWs. Typically, the energy in these waves is a few times smaller than the energy in high-energy electrons.

In the burster frame, a magnetized wind flows away from the burster at relativistic speeds and collides with an ambient medium. In the process of such a collision, the outflowing wind loses its energy. From the listed results of our simulations of the beam – barrier collision (Smolsky & Usov 1996, Usov & Smolsky 1998), it follows that at  $r \sim r_{\text{dec}}$ , where  $\alpha$  is  $\sim 1$ , about 70% of the energy losses of the wind are transferred to protons of the ambient medium which are reflected from the wind front. The mean energy of reflected protons is about  $m_p c^2 \Gamma_0^2$ . The other 30% of the wind energy losses are distributed between high-energy electrons and LAEMWs. As a rule, the total energy in accelerated electrons is a few times higher than the total energy in LAEMWs.

High-energy electrons accelerated at the wind front generate non-thermal radiation while they move in both the magnetic field of the wind and the electromagnetic fields of LAEMWs that propagate ahead of the wind front. Let us consider this radiation.

### 5.1. Synchrotron radiation from the wind front

In our simulations of the beam – magnetic barrier interaction (Smolsky & Usov 1996, Usov & Smolsky 1998), the examined space-time domain is

$$x_{\min} < x < x_{\max}, \quad 0 < t < t_{\max}, \quad (15)$$

where  $x_{\max}$  and  $-x_{\min}$  are equal to a few  $\times(1-10)(c/\omega_{Bp})$ ,  $t_{\max}$  is equal to a few  $\times(1-10)T_p$ , and  $(c/\omega_{Bp})$  is the proton gyroradius in the magnetic field of the barrier  $B_0$ . Non-thermal radiation of high-energy electrons from the examined space domain was calculated for the beam and barrier parameters which are relevant to cosmological GRBs (Smolsky & Usov 1996, Usov & Smolsky 1998). Figure 3 shows the intensity of radiation as a function of time  $t$  for a simulation with  $B_0 = 300$  G,  $\Gamma_0 = 300$ ,  $\alpha = 2/3$ ,  $x_{\min} = -5(c/\omega_{Bp})$  and  $x_{\max} = 30(c/\omega_{Bp})$ . In all our simulations, the bulk of calculated radiation is generated via synchrotron mechanism in a compact vicinity,  $x_{\text{pen}} - 2(c/\omega_{Bp}) < x < x_{\text{pen}}$ , of the barrier front where both the strength of the magnetic field is of the order of  $B_0$  and the mean energy of accelerated electrons is extremely high. Radiation of high-energy electrons in the fields of LAEMWs is negligible ( $\sim 1\%$  or less) because both the fields of these waves are about an order of magnitude smaller than  $B_0$  (see below) and the length of the examined space domain (15) is restricted for computational reasons.

At  $\alpha \sim 1$ , the mean energy of synchrotron photons generated at the front of the barrier is

$$\langle \varepsilon_\gamma \rangle \simeq 0.1 \left( \frac{\Gamma_0}{10^2} \right)^2 \left( \frac{B_0}{10^3 \text{ G}} \right) \text{ MeV}. \quad (16)$$

The average fraction of the kinetic energy of the beam that is radiated in these photons is

$$\xi_\gamma \equiv \frac{\langle \Phi_\gamma \rangle}{n_0 m_p c^3 \Gamma_0} \simeq 10^{-3} \left( \frac{\Gamma_0}{10^2} \right)^2 \left( \frac{B_0}{10^3 \text{ G}} \right), \quad (17)$$

where  $\langle \Phi_\gamma \rangle$  is the average synchrotron luminosity of high-energy electrons per unit area of the barrier front.

In the burster frame, the characteristic energy,  $\langle \tilde{\varepsilon}_\gamma \rangle$ , of synchrotron photons generated in the vicinity of the wind front increases due to the Doppler effect. Taking this into account and using equation (16), we have

$$\langle \tilde{\varepsilon}_\gamma \rangle \simeq 10 \left( \frac{\Gamma_0}{10^2} \right)^2 \left( \frac{B_{\text{dec}}}{10^5 \text{ G}} \right) \text{ MeV}. \quad (18)$$

The fraction of the wind energy which is transferred to radiation at the wind front does not depend on the frame where it is estimated, and in the burster frame it is equal to

$$\tilde{\xi}_\gamma = \xi_\gamma \simeq 10^{-3} \left( \frac{\Gamma_0}{10^2} \right) \left( \frac{B_{\text{dec}}}{10^5 \text{ G}} \right), \quad (19)$$

For typical parameters of relativistic magnetized winds which are relevant to cosmological  $\gamma$ -ray bursters,  $\Gamma_0 \simeq 10^2 - 10^3$  and  $B_{\text{dec}} \simeq 10^5 \text{ G}$ , from equations (18) and (19) we have  $\langle \tilde{\varepsilon}_\gamma \rangle \simeq 10 - 10^3 \text{ MeV}$  and  $\tilde{\xi} \simeq 10^{-2} - 10^{-3}$ . Hence, the synchrotron radiation that is generated at wind front may be responsible for high-energy  $\gamma$ -rays that are observed in the spectra of some GRBs (e.g., Hurley et al. 1994).

The main part of the X-ray and  $\gamma$ -ray emission of detected GRBs is in the BATSE range, from a few  $\times 10 \text{ keV}$  to a few MeV (e.g., Fishman & Meegan 1995). Synchrotron radiation from the wind front is either too hard or too weak to explain this emission irrespective of  $B_{\text{dec}}$ . Indeed, equations (18) and (19) yield

$$\langle \tilde{\varepsilon}_\gamma \rangle \simeq 10^2 \left( \frac{\Gamma_0}{10^2} \right) \left( \frac{\tilde{\xi}_\gamma}{10^{-2}} \right) \text{ MeV}. \quad (20)$$

In our model, the energy of rotation powered winds which are responsible for cosmological GRBs cannot be significantly more than  $10^{53}$  ergs. To explain the energy output of  $\sim 10^{51} - 10^{53}$  ergs per GRB, the efficiency of transformation of the wind energy into the energy of non-thermal radiation must be more than 1%,  $\tilde{\xi}_\gamma > 10^{-2}$ , and maybe, for some GRBs it is as high as 100%,  $\tilde{\xi}_\gamma \simeq 1$ . Taking into account that for cosmological GRBs the value of  $\Gamma_0$  is  $> 10^2$  (e.g., Fenimore et al. 1993, Baring & Harding 1997), for  $\tilde{\xi}_\gamma > 10^{-2}$  from equation (20) it follows that the mean energy of synchrotron photons generated at the wind front is very high,  $\langle \tilde{\varepsilon}_\gamma \rangle > 100 \text{ MeV}$ . This is because the bulk of these photons is generated in the thin vicinity of the wind front where there are both a strong magnetic field,  $B \simeq B_0$ , and high-energy electrons. The mean time that high-energy electrons spend in this vicinity and generate synchrotron radiation is very short,  $\sim$  a few  $\times T_p \sim 10^{-6} (B_{\text{dec}}/10^5 \text{ G})^{-1} (\Gamma_0/10^2) \text{ s}$ . To get a high efficiency of synchrotron radiation at the wind front,  $\tilde{\xi}_\gamma > 10^{-2}$ , it is necessary to assume that the magnetic field  $B_{\text{dec}}$  is about its maximum value,  $B_{\text{dec}} \sim 10^6 \text{ G}$ . From equation (18), we can see that in this case the mean energy of synchrotron photons is of the order of or higher than  $10^2 \text{ MeV}$ .

For a typical value of  $B_{\text{dec}}$ , that is  $\sim 10^5 \text{ G}$ , and  $\Gamma_0 \sim 10^2 - 10^3$ , from equation (19) we have  $\tilde{\xi}_\gamma \sim 10^{-3} - 10^{-2} \ll 1$ . Hence, electrons of the ambient medium are accelerated at the wind front and injected into the region ahead of the front practically without energy losses. In our model, these high-energy electrons are the best candidates to be responsible for the X-ray and  $\gamma$ -ray emission of GRBs in the BATSE range.

## 5.2. LAEMWs generated at the wind front

At  $\alpha \sim 1$ , LAEMWs are generated at the wind front and propagate in both directions from the front (see Fig. 2). These waves are non-monochromatic. Figure 4 shows a typical spectrum of LAEMWs in the wind frame. This spectrum has a maximum at the frequency  $\omega_{\text{max}}$  which is a few times higher than the proton gyrofrequency  $\omega_{Bp} = eB_0/m_p c \Gamma_0$  in the field of  $B_0$ .

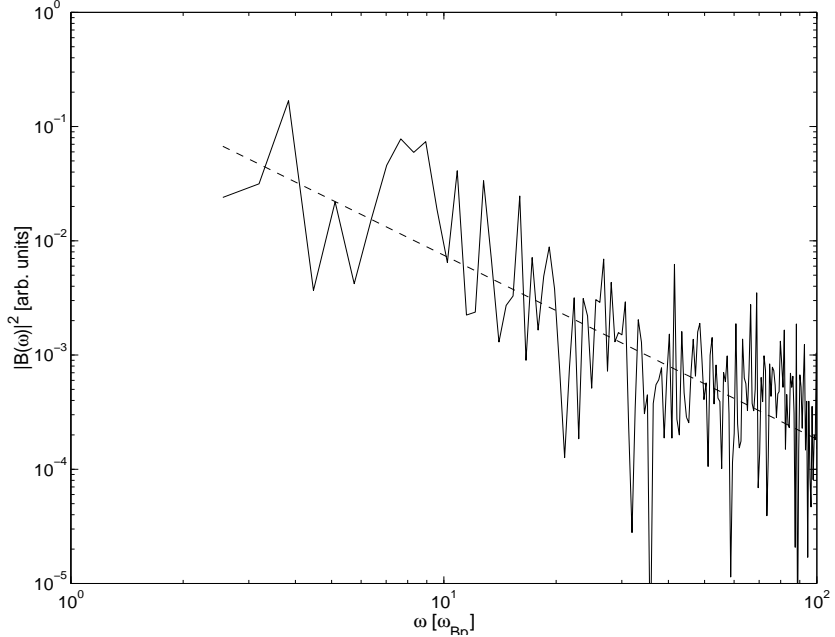


Figure 4. Power spectrum of LAEMWs (thin line) generated at the front of the magnetic barrier in a simulation with  $B_0 = 300$  G,  $\Gamma_0 = 300$  and  $\alpha = 2/3$ . The spectrum is fitted by a power law (dotted line).

At high frequencies,  $\omega > \omega_{\max}$ , the spectrum of LAEMWs may be fitted by a power law:

$$|B(\omega)|^2 \propto \omega^{-\beta}, \quad (21)$$

where  $\beta \simeq 1.6$ .

The mean field of LAEMWs depends on  $\alpha$ , and in the wind frame, for  $\alpha_{\text{cr}} < \alpha < 1$  this field is

$$\langle B_w \rangle = (\langle B_z \rangle^2 + \langle E_y \rangle^2)^{1/2} \simeq 0.1B_0 \simeq 0.1B_{\text{dec}}/\Gamma_0 \quad (22)$$

within a factor of 2 or so.

### 5.3. High-energy electrons accelerated at the wind front

At  $r \sim r_{\text{dec}}$ , where  $\alpha$  is  $\sim 1$ , about 20 % of the energy of a relativistic strongly magnetized wind is transferred to electrons of the ambient medium which are reflected from the wind front and accelerated to extremely high energies (Smolsky & Usov 1996, 1999, Usov & Smolsky 1998). In the wind frame, the spectrum of high-energy electrons in the region ahead of the wind front may be fitted by a two-dimensional relativistic Maxwellian (Smolsky & Usov 1999)

$$\frac{dn_e}{d\Gamma_e} \propto \Gamma_e \exp\left(-\frac{m_e c^2 \Gamma_e}{kT}\right) \quad (23)$$

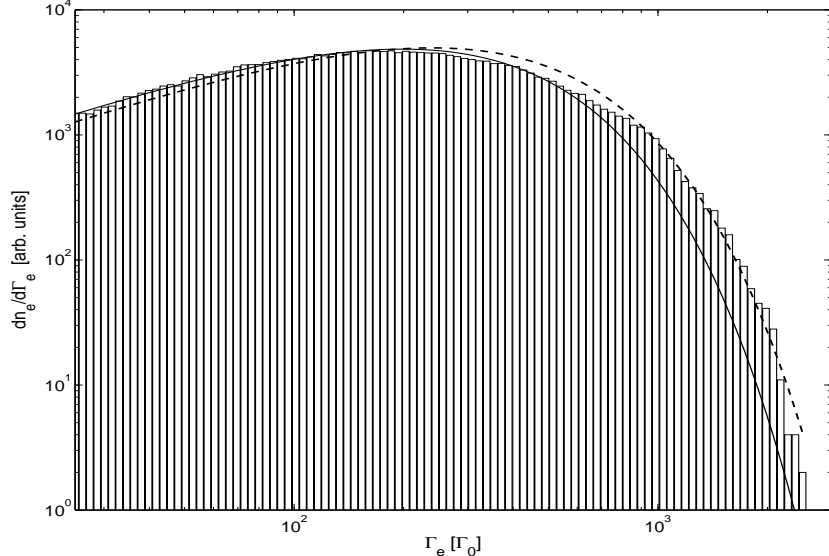


Figure 5. Energy spectrum of highly accelerated electrons in the region ahead of the wind front in the frame of the wind for a simulation with  $B_0 = 300$  G,  $\Gamma_0 = 300$  and  $\alpha = 2/3$ . The electron spectrum is fitted by a two-dimensional relativistic Maxwellian with a relativistic temperature  $T = m_e c^2 \Gamma_T / k$ , where  $\Gamma_T$  is equal to either  $240\Gamma_0$  (dotted line) or  $200\Gamma_0$  (solid line).

with a relativistic temperature  $T = m_e c^2 \Gamma_T / k$ , where  $\Gamma_T \simeq 240\Gamma_0$  (Fig. 5). The fact that the energy distribution of accelerated electrons at  $\alpha \sim 1$  is close to a relativistic Maxwellian is quite natural because at  $\alpha > \alpha_{\text{cr}}$  the trajectories of particles in the front vicinity are fully chaotic. The thermal distribution of high energy electrons does not come as a result of interparticle collisions, since the ambient medium is collisionless and no artificial viscosity is included in the simulation code (Smolsky & Usov 1996). Thermalization of the electron distribution is purely a result of collisionless interactions between particles and electromagnetic oscillations generated at the wind front.

At  $\Gamma_e \leq 700\Gamma_0$ , the fit of the electron spectrum with a two-dimensional relativistic Maxwellian (23) with  $\Gamma_T \simeq 200\Gamma_0$  is rather accurate (Fig. 5). In this case, a small excess of electrons with Lorentz factors  $\Gamma_e > 700\Gamma_0$  may be interpreted as a high-energy tail. Such a tail may result, for example, from multiple acceleration of high-energy electrons at the wind front. The angular distribution of high-energy electrons in the region far ahead of the wind front is anisotropic. The mean angle between the velocity of outflowing electrons and the normal to the wind front is  $\langle \psi \rangle \simeq 1/3$  radian.

#### 5.4. Synchro-Compton radiation of high-energy electrons from the region ahead of the wind front

High-energy electrons with a nearly Maxwellian spectrum are injected into the region ahead of the wind front and radiate in the fields of LAEMWs via synchro-

Compton mechanism. For  $\langle\psi\rangle \simeq 1/3$ , synchro-Compton radiation of high-energy electrons closely resembles synchrotron radiation (e.g. Blumenthal & Tucker 1974, Smolsky & Usov 1999). Therefore, to model the spectrum of synchro-Compton radiation, we replace the fields of LAEMWs  $B_z(t, x)$  and  $E_y(t, x)$  by a constant magnetic field which is equal to the mean field of LAEMWs  $\langle B_w \rangle$ . The energy losses of electrons in such a magnetic field are governed by (Landau & Lifshitz 1971)

$$\frac{d\Gamma_e}{dt} = -\chi(\Gamma_e^2 - 1), \quad (24)$$

where  $\chi = 2e^4\langle B_w \rangle^2/3m_e^3c^5$ .

In our approximation, the evolution of the spectrum of high-energy electrons in the region ahead of the wind front may be found from the following equation (e.g., Pacholczyk 1969)

$$\frac{\partial f(\Gamma_e, t)}{\partial t} = \frac{\partial}{\partial \Gamma_e} [\chi \Gamma_e^2 f(\Gamma_e, t)] + \dot{N}_e f_{\text{bar}}(\Gamma_e), \quad (25)$$

where  $f(\Gamma_e, t)$  is the distribution function of high-energy electrons in the region ahead of the wind front per unit area of the front at the moment  $t$ ,  $\dot{N}_e \simeq n_0 c$  is the rate of production of high-energy electrons per unit area of the front, and  $f_{\text{bar}} = (\Gamma_e/\Gamma_T^2) \exp(-\Gamma_e/\Gamma_T)$  is the average spectrum of high-energy electrons which are injected into the region ahead of the front. The function  $f(\Gamma_e, t)$  is normalized to the total number of high-energy electrons per unit area of the front  $N_e$ , while the function  $f_{\text{bar}}$  is normalized to unity:

$$\int_1^\infty f(\Gamma_e, t) d\Gamma_e = N_e \quad \text{and} \quad \int_1^\infty f_{\text{bar}} d\Gamma_e = 1. \quad (26)$$

For simplicity, we disregard the angular anisotropy of the electron distribution.

Under the mentioned assumptions, in the frame of the wind front the differential proper intensity of synchro-Compton radiation from the region ahead of the wind front is (e.g., Pacholczyk 1969, Rybicki & Lightman 1979)

$$I_\nu(t) = \int_1^\infty f(\Gamma_e, t) i_\nu d\Gamma_e, \quad (27)$$

where

$$i_\nu = \frac{\sqrt{3}e^3\langle B_w \rangle}{m_e c^2} \frac{\nu}{\nu_c} \int_{\nu/\nu_c}^\infty K_{5/3}(\eta) d\eta, \quad (28)$$

is the spectrum of synchrotron radiation generated by a single relativistic electron in a uniform magnetic field  $\langle B_w \rangle$ ,  $K_{5/3}$  is the modified Bessel functions of 5/3 order and

$$\nu_c = \frac{3e\langle B_w \rangle \Gamma_e^2}{4\pi m_e c} \quad (29)$$

is the typical frequency of synchrotron radiation.

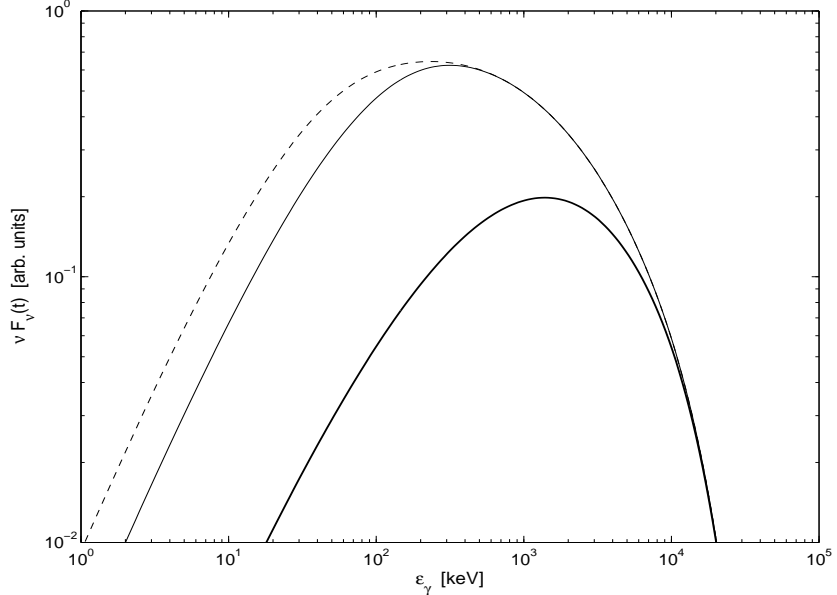


Figure 6. Calculated spectral power of synchro-Compton radiation from the region ahead of the wind front as a function of photon energy for  $\Gamma_0 = 150$ ,  $B_0 = 300$  G,  $\langle B_w \rangle = 0.1B_0$ ,  $\Gamma_T = 200\Gamma_0 = 3 \times 10^4$  and  $z = 1$ . The spectrum of radiation is given for the moments when the fraction of the energy of high-energy electrons injected into the region ahead of the wind front which is radiated is very small,  $\ll 1\%$  (thick solid line), 36% (thin solid line) and 58% (dotted line).

The observed spectral flux  $F_\nu(t)$  (in units  $\text{erg s}^{-1} \text{cm}^{-2} \text{erg}^{-1}$ ) can be obtained from the proper intensity  $I_\nu(t)$  dividing by the square of the burster distance  $d$ , and by taking into account both the effects of relativistic beaming and cosmological effects (e.g., Tavani 1996a, Dermer 1998):

$$F_\nu(t) = \frac{D^3(1+z)}{4\pi d^2} I_{\nu'}(t), \quad (30)$$

where  $D$  is the relativistic Doppler factor,  $D \simeq 2\Gamma_0$ , and  $z$  is the cosmological redshift. The observed frequency  $\nu$  depends on the emitted frequency  $\nu'$  in the wind frame as  $\nu = [D/(1+z)]\nu' \simeq [2\Gamma_0/(1+z)]\nu'$ .

Equations (24) - (30) were integrated numerically. For typical parameters of cosmological  $\gamma$ -ray bursters,  $\Gamma_0 = 150$ ,  $B_0 = 300$  G,  $\langle B_w \rangle = 0.1B_0$ ,  $\Gamma_T = 200\Gamma_0 = 3 \times 10^4$  and  $z = 1$ , Figure 6 shows the observed spectrum of synchro-Compton radiation from the region ahead of the wind front. For this radiation, the characteristic energy of photons is in the BATSE range (Band et al. 1993, Schaefer 1994, 1998, Fishman & Meegan 1995, Preece et al. 1996). The spectrum of synchro-Compton radiation displays a continuous hard to soft evolution, in agreement with observational data on GRBs (Bhat et al. 1994).

To fit the observed spectra of GRBs, for accelerated electrons it was usually taken either a three-dimensional relativistic Maxwellian distribution (Katz

1994a,b) or a sum of a three-dimensional relativistic Maxwellian distribution and a suprathermal power-law tail (Tavani 1996a,b). The thermal character of the electron distribution (or its part) is consistent with our results (see § 5.3). In our simulations, we observe a two-dimensional relativistic Maxwellian distribution of accelerated electrons. However, the difference between 2D and 3D Maxwellian distributions does not change the calculated spectrum of synchrotron radiation significantly (Jones & Hardee 1979, Rybicki & Lightman 1979).

In many papers (see, for a review Piran 1998), the interaction of a relativistic wind with an ambient medium and non-thermal radiation generated at  $r \sim r_{\text{dec}}$  were considered in the frame of the conventional model which was based on the following assumptions.

- (1) Two collisionless shocks form: an external shock that propagates from the wind front into the ambient medium, and an internal shock that propagates from the wind front into the inner wind, with a contact discontinuity at the wind front between the shocked material.
- (2) Electrons are accelerated at the shocks to very high energies.
- (3) The shocked matter acquires embedded magnetic fields. The energy density of these fields is about the energy density of high-energy electrons accelerated at the shocks.
- (4) Highly accelerated electrons generate high-frequency (X-ray and  $\gamma$ -ray) radiation of GRBs via synchrotron mechanism.
- (5) The efficiency of conversion of the wind energy into accelerated electrons and then to high-frequency radiation of GRBs is about 10%  $\sim$  30%.

The idea about formation of two collisionless shocks near the front of a relativistic wind outflowing from a cosmological  $\gamma$ -ray burster is based mainly on both theoretical studies which have shown that collisionless shocks can form in a rarified plasma (e.g., Tidman & Krall 1971, Dawson 1983, Quest 1985) and the fact that such shocks have been observed in the vicinities of a few comets and planets (e.g., Leroy et al. 1982, Livesey, Kennel & Russell 1982, Omid & Winske 1990). Undoubtedly, collisionless shocks exist and can accelerate electrons to ultrarelativistic energies in many astrophysical objects such as supernova remnants and jets of active galactic nuclei. However, for the wind parameters which are relevant to cosmological GRBs (see § 2), formation of collisionless shocks in the vicinity of the wind front is very questionable, especially if  $\Gamma_0$  is as high as  $10^3$  or more (e.g., Smolsky & Usov 1996, 1999, Mitra 1996, Brainerd 1999). As to an internal shock, it cannot form in a Poynting flux-dominated wind, in principle (e.g., Kennel, Fujimura & Okamoto 1983, Kennel & Coroniti 1984).

Our model of the wind – ambient medium interaction qualitatively differs from the conventional model which is based on the assumption that an external collisionless shock forms just ahead of the wind front. Although it might seem that observational consequences of our model must differ from observational consequences of the conventional model significantly, this is not the case. Moreover, we can see that all the listed assumptions of the conventional model except of the first one are confirmed by our simulations. There is only a modification that LAEMWs are embedded in the region ahead of the wind front instead of magnetic fields, and highly accelerated electrons generate high-frequency emission of GRBs via synchro-Compton radiation. However, in our case synchro-Compton radiation closely resembles synchrotron radiation. Therefore, if in the conven-

tional model of GRB emission from the shocked region ahead of the wind front the mechanism of electron acceleration by a relativistic collisionless shock is replaced by the mechanism of electron acceleration at the wind front, this model will remain otherwise practically unchanged.

At  $r > r_{\text{dec}}$ , the outflowing wind slows down due to its interaction with the ambient medium, and when the Lorentz factor of the wind front is about several tens or less, an external shock may form just ahead of the front. We believe that the afterglows which are observed in  $\sim 10^5$  s after some GRBs result from acceleration of electrons by such shocks as it is generally accepted (Mészáros & Rees 1997b, Vietri 1997, Waxman 1997, Wijers, Rees & Mészáros 1997).

**Acknowledgments.** This research was supported by MINERVA Foundation, Munich / Germany.

## References

- Band, D., et al. 1993, ApJ, 413, 281  
Baring, M.G., & Harding, A.K. 1997, ApJ, 491, 663  
Benford, G. 1984, ApJ, 282, 154  
Bhat, P.N. et al. 1994, ApJ, 426, 604  
Blackman, E.G. & Yi, I. 1998, ApJ, 498, L31  
Blackman, E.G., Yi, I., & Field, G.B. 1996, ApJ, 473, L79  
Blandford, R.D., & Eichler, D. 1987, Phys. Rep., 154, 1  
Blaes, O.M. 1994, ApJS, 92, 643  
Blumenthal, G.R. & Tucker, W.H. 1974, in X-Ray Astronomy, R. Giacconi and H. Gursky, Dordrecht: Reidel, 99  
Brainerd, J.J. 1999, astro-ph/9904040  
Coroniti, F.V. 1990, ApJ, 349, 538  
Dai, Z.G., & Lu, T. 1998, A&A, 333, L87  
Dawson, J.M. 1983, Rev. Mod. Phys., 55, 403  
Dermer, C.D. 1998, ApJ, 501, L157  
Dermer, C.D., & Weiler, T.J. 1995, Ap&SS, 231, 377  
Eichler, D., Livio, M., Piran, T. & Schramm, D. 1989, Nature, 340, 126  
Fenimore, E.E., Epstein, R.I., & Ho, C. 1993, A&AS, 97, 59  
Fishman, G.J. & Meegan, C.A. 1995, ARA&A, 33, 415  
Gaensler, B.M., Brazier, K.T.S., Manchester, R.N., & Johnston, S. 1999, astro-ph/9901262  
Goodman, J. 1986, ApJ, 308, L47  
Goodman, J., Dar, A., & Nussinov, S. 1987, ApJ, 314, L7  
Greiner, J. 1998, astro-ph/9802222  
Gunn, J.E. & Ostriker, J.P. 1971, ApJ, 165, 223  
Harding, A.K. 1994, ApJS, 90, 863

- Hartmann, D. 1995, in *The Gamma-Ray Sky with Compton GRO and SIGMA*, NATO ASI Proc. 461, ed. M. Signore, P. Salati, & G. Vedrenne, Dordrecht: Kluwer, 329
- Herster, J.J. 1998, in *Neutron Stars and Pulsars: Thirty Years after the Discovery*, N. Shibasaki, N. Kawai, S. Shibata, & T. Kifune, Tokyo: Universal Academy Press, 431
- Hurley, K., et al. 1994, *Nature*, 372, 652
- Janka, H.-Th., & Ruffert, M. 1996, *A&A*, 1996, 307, L33
- Jones, T.W., & Hardee, P.E. 1979, *ApJ*, 228, 268
- Katz, J. 1994a, *ApJ*, 432, L107
- Katz, J. 1994b, in *Gamma-Ray Bursts, Second Workshop*, G.J. Fishman, J.J. Brainerd, & K. Hurley, New York: AIP, 529
- Katz, J. 1997, *ApJ*, 490, 633
- Kennel, C.F., & Coroniti F.V. 1984, *ApJ*, 283, 694
- Kennel, C.F., Fujimura, F.S., & Okamoto, I. 1983, *J. Ap. Geophys. Fluid Dyn.*, 26, 147
- Kluźniak, W., & Ruderman, M. 1998, *ApJ*, 505, L113
- Kulkarni, S.R., et al. 1998, *Nature*, 393, 35
- Kulkarni, S.R., et al. 1999, *Nature*, 398, 389
- Landau, L.D., & Lifshitz, E.M. 1971, *The Classical Theory of Fields*, Elmsford: Pergamon Press
- Leroy, M.M., Winske, D., Goodrich, C.C., Wu, C.S., & Papadopoulos, K. 1982, *J. Geophys. Res.*, 87, 5081
- Lipunov, V.M., Postnov, K.A., Prokhorov, M.E., Panchenko, I.E., & Jorgensen, H.E. 1995, *ApJ*, 454, 593
- Livesey, W.A., Kennel, C.F., & Russell, C.T. 1982, *Geophys. Res. Lett.*, 9, 1037
- Meegan, C.A., Fishman, G.J., Wilson, R.B., Paciasas, W.S., Pendleton, G.N., Horack, J.M., Brock, M.N., & Kouveliotou, C. 1992, *Nature*, 355, 143
- Meegan, C.A., et al. 1994, in *Gamma-Ray Bursts, Second Workshop*, G.J. Fishman, J.J. Brainerd, & K. Hurley, New York: AIP, 3
- Melatos, A. & Melrose, D.B. 1996a, *MNRAS*, 279, 1168
- Melatos, A. & Melrose, D.B. 1996b, *ASP Conf. Ser.*, 105, 421
- Mészáros, P., & Rees, M.J. 1992, *ApJ*, 397, 570
- Mészáros, P., & Rees, M.J. 1993, *ApJ*, 405, 278
- Mészáros, P., & Rees, M.J. 1997a, *ApJ*, 482, L29
- Mészáros, P., & Rees, M.J. 1997b, *ApJ*, 476, 232
- Metzger, R.M. et al. 1997, *Nature*, 387, 879
- Michel, F.C. 1971, *Comments Ap. Space Phys.*, 3, 80
- Michel, F.C. 1985, *ApJ*, 288, 138
- Mitra, A. 1996, *A&A*, 313, L9
- Narayan, R., Paczyński, B., & Piran, T. 1992, *ApJ*, 395, L83
- Omid, N., & Winske, D. 1990, *J. Geophys. Res.*, 95, 2281
- Pacholczyk, A.G. 1969, *Radio Astrophysics*, San Francisco: Freeman

- Paczynski, B. 1986, ApJ, 308, L43
- Paczynski, B. 1990, ApJ, 363, 218
- Paczynski, B. 1991, Acta Astron., 41, 257
- Padilla, L., et al. 1998, A&A, 337, 43
- Perna, R., & Loeb, A. 1998, ApJ, 509, L85
- Piran, T. 1998, astro-ph/9810256
- Preece, R.D., et al. 1996, ApJ, 473, 310
- Quest, K.B. 1985, Phys. Rev. Lett., 54, 1872
- Rees, M.J., & Mészáros, P. 1992, MNRAS, 258, 41
- Rybicki, G.B., & Lightman, A.P. 1979, Radiative Processes in Astrophysics, New York: Wiley
- Schaefer, B.E., et al. 1994, ApJS, 92, 285
- Schaefer, B.E., et al. 1998, ApJ, 492, 696
- Smolsky, M.V., & Usov, V.V. 1996, ApJ, 461, 858
- Smolsky, M.V., & Usov, V.V. 1999, ApJ, submitted
- Sulkanen, M.E., & Lovelace, R.V.E. 1990, ApJ, 350, 732
- Tamblyn, P., & Melia, F. 1993, ApJ, 417, 421
- Tavani, M. 1996a, ApJ, 466, 768
- Tavani, M. 1996b, Phys. Rev. Lett., 76, 3478
- Thompson, C., & Duncan, R.C. 1993, ApJ, 408, 194
- Tidman, D.A., & Krall, N.A. 1971, Shock waves in collisionless plasma, New York: Wiley
- Usov, V.V. 1975, Ap&SS, 32, 375
- Usov, V.V. 1992, Nature, 357, 472
- Usov, V.V. 1994a, MNRAS, 267, 1035
- Usov, V.V. 1994b, in Gamma-Ray Bursts, Second Workshop, G.J. Fishman, J.J. Brainerd, & K. Hurley, New York: AIP, 552
- Usov, V.V., & Chibisov, G.V. 1975, Soviet Astron., 19, 115
- Usov, V.V., & Smolsky, M.V. 1998, Phys. Rev. E, 57, 2267
- van den Berg, S. 1983, Ap&SS, 97, 385
- Vietri, M. 1996, ApJ, 471, L95
- Vietri, M. 1997, ApJ, 478, L9
- Waxman, E. 1997, ApJ, 485, L5
- Wickramasinghe, W.A.D.T., Nemiroff, R.J., Norris, J.P., Kouveliotou, C., Fishman, G.J., Meegan, C.A., Wilson, R.B., & Paciesas, W.S. 1993, ApJ, 411, L55
- Wijers, R.A.M.J., Rees, M.J., & Mészáros, P. 1997, MNRAS, 288, 51P
- Woosley, S.E. 1993, A&A, 97, 205
- Yi, I., & Blackman, E.G. 1998, ApJ, 494, L163